Decay cascades of acoustic phonons in calcium fluoride

1989 J. Phys.: Condens. Matter 1 8809

(http://iopscience.iop.org/0953-8984/1/45/006)

J. Phys.: Condens. Matter **1** (1989) 8809–8822. Printed in the UK

Decay cascades of acoustic phonons in calcium fluoride

M T Labrot†, A P Mayer†, R K Wehner† and P E Obermayer‡

† Institut für Theoretische Physik II, Westfälische Wilhelms-Universität Münster, 4400 Münster, Federal Republic of Germany

‡ Institut für Angewandte Physik, Universität Regensburg, 8400 Regensburg, Federal Republic of Germany

Received 31 January 1989

Abstract. The temporal evolution of a spatially homogeneous non-equilibrium distribution of non-dispersive acoustic phonons is investigated for small occupation numbers in the presence of impurities as incoherent elastic scatterers. The phonon–phonon interaction governing the spontaneous decay via cubic anharmonicity is accounted for quantitatively on the basis of non-linear elasticity theory. The theoretical results are compared with the experimental data of Happek *et al*.

1. Introduction

The relaxation of phonon systems from states far from equilibrium has gained increasing interest during recent years and has been studied by various experimental and theoretical methods. In general, the relaxation processes depend on the initial conditions as well as on the details of the phonon–phonon interactions and interactions with impurities. In many cases, three-phonon processes due to cubic anharmonicity and elastic scattering by impurities including mode conversion may be considered as most important for the changes of the phonon occupation numbers in space and time [1]. In crystals at sufficiently low temperatures, after an initial period only the acoustic phonons play a role in the relaxation towards thermal equilibrium. While in the beginning the spontaneous decay, leading to cascades, is dominant (down-conversion), in the final stages the phonon–phonon scattering (up-conversion) also becomes important. Both processes can be treated satisfactorily in a quantitative manner on the basis of cubic anharmonicity.

Transport equations, which govern the temporal and spatial evolution of the phonon occupation numbers in situations involving decay cascades, have been established and analysed in detail by Levinson and co-workers [2–8], and also by Schaich [9] and Wilson and Schaich [10]. In particular, Kazakovtsev and Levinson [3] have shown that the phonon occupation numbers obey a scaling law as functions of time, space and frequency. Their results are mainly of a qualitative nature, since the detailed form of the phonon–phonon interaction has not been taken into account. In a frequency regime, where the dispersion can largely be neglected, the relaxation processes can be assessed quantitatively, because it bears the advantage that the anharmonic coupling coefficients are completely determined by the second- and third-order elastic moduli, and no lattice-dynamical models have to be invoked.

0953-8984/89/458809 + 14 $02.50

Happek *et al* [11, 12] have studied experimentally decay cascades of acoustic phonons in the system $CaF_2:Eu^{2+}$ under spatially homogeneous conditions with no resolution of the propagation directions. For this system, they have rederived and experimentally confirmed the scaling law. The temporal behaviour of the phonon occupation numbers has then been determined by rate equations, into which the phonon–phonon interaction enters only via characteristic functions. For a quantitative comparison of their experimental results with the solution of the rate equations, Happek *et al* have used an *ad hoc* ansatz for the characteristic functions, the detailed behaviour of which is unknown so far. We have calculated these functions numerically for CaF_2 on the basis of non-linear elasticity theory, taking full account of the anisotropy and of the anharmonicity by using the experimentally known elastic constants of second and third order. As an initial condition for the relaxation process under consideration, we assume an incoherent non-equilibrium distribution of monochromatic phonons. For comparison with the available experimental data we have evaluated the rate equations of the phonon occupation numbers only with respect to averages over the propagation directions. The averaged phonon occupation numbers then depend only on the time, on the frequency and on the phonon branch. The phonon–phonon interactions enter the rate equations in the form of frequency-dependent and branch-dependent characteristic functions.

For isotropic non-linear elastic media, which have been studied earlier numerically [13], the characteristic functions are given by analytic expressions. While the strength of the anharmonic coupling is completely determined in the present theory and no parameters had to be adjusted for agreement with experiment, the strength of the impurity scattering is actually not precisely known. In the long-wavelength limit, the scattering rate is proportional to the fourth power of the frequency. In our numerical study of the time behaviour of the phonon distribution function, we assume incoherent elastic scattering at mass defects with one free parameter. For a comparison with the experimental data of references [11] and [12], it is adequate to assume that the impurity scattering is very fast compared with the three-phonon processes. In this limit the spectral distribution of the total energy has been calculated by summation over the phonon branches.

2. Dynamics of acoustic phonons in non-equilibrium

In this paper the rate equations for the acoustic phonons are studied under special assumptions. The crystal is considered to be at zero temperature and the incoherently excited phonons are assumed to be homogeneously distributed in space. The occupation numbers of the acoustic phonons are treated as small compared with one, and consequently Peierls' collision operator has been linearised. Instead of the number $n_{qj}(t)$ of phonons with wavevector $\boldsymbol{q}$ belonging to branch j, we use as dynamic variable the number of phonons per units of volume, of frequency interval and of solid angle

$$f_{\hat{q}j}(\nu, t) = (\nu^2/v_{\hat{q}j}^3)n_{qj}(t) \tag{2.1}$$

which we call the phonon distribution function. Here, $\hat{\boldsymbol{q}}$ denotes the unit vector in the propagation direction and $v_{\hat{q}j}$ denotes the phase velocity. For this quantity the phonon transport equation can be written under the above assumptions in the form

$$\dot{f}_{\hat{q}j}(\nu, t) = -2\nu^5\gamma_{\hat{q}j}f_{\hat{q}j}(\nu, t) + \sum_{j'}\int \mathrm{d}\Omega' \int \mathrm{d}\nu'\gamma(\nu/\nu', \hat{\boldsymbol{q}}j, \hat{\boldsymbol{q}}'j')\nu'^4 f_{\hat{q}'j'}(\nu', t)$$

$$- \nu^4 M_{\hat{q}j}f_{\hat{q}j}(\nu, t) + \sum_{j'}\int \mathrm{d}\Omega' M(\hat{\boldsymbol{q}}j, \hat{\boldsymbol{q}}'j')\nu^4 f_{\hat{q}'j'}(\nu, t). \tag{2.2}$$

The terms on the right-hand side take into account phonon decay and defect scattering. Each process is characterised by a gain and a loss term. According to the dynamic theory of interacting phonons, the decay via cubic anharmonicity contributes to the quantities $\gamma(\nu/\nu', \hat{\boldsymbol{q}}j, \hat{\boldsymbol{q}}'j')$ in (2.2) the following terms:

$$\gamma(\nu/\nu', \hat{\boldsymbol{q}}j, \hat{\boldsymbol{q}}'j') = \sum_{j''} \gamma(\nu/\nu', \hat{\boldsymbol{q}}'j' \rightarrow \hat{\boldsymbol{q}}j + \widehat{(\hat{\boldsymbol{q}}' - \boldsymbol{k})}j'') \tag{2.3}$$

where $\boldsymbol{k} = (\nu/\nu')(v_{\hat{\boldsymbol{q}}'j'}/v_{\hat{\boldsymbol{q}}j})\hat{\boldsymbol{q}}$ and

$$\gamma(\nu/\nu', \hat{\boldsymbol{q}}'j' \rightarrow \hat{\boldsymbol{q}}j + \widehat{\hat{\boldsymbol{q}}' - \boldsymbol{k}}j'') = (\nu^2/\nu'^2)[(2\pi)^3 V/v_{\hat{\boldsymbol{q}}j}^3 v_{\hat{\boldsymbol{q}}'j'}^2] \times |V_3(-\hat{\boldsymbol{q}}'j', \boldsymbol{k}j, \hat{\boldsymbol{q}}' - \boldsymbol{k}j'')|^2 \delta(v_{\hat{\boldsymbol{q}}'j'} - kv_{\hat{\boldsymbol{k}}j} - |\hat{\boldsymbol{q}}' - \boldsymbol{k}| v_{\hat{\boldsymbol{q}}' - \boldsymbol{k}j''}). \tag{2.4}$$

V denotes the crystal volume. The quantity $\gamma_{\hat{\boldsymbol{q}}j}\nu^5$ is the imaginary part of the phonon self-energy at the frequency ν. The phonon lifetime is given by $\tau = 1/(2\gamma_{\hat{\boldsymbol{q}}j}\nu^5)$. The ν^5-dependence of the lifetime of spontaneously decaying acoustic phonons has been observed experimentally for the first time by Baumgartner *et al* [14]. The reduced damping constants $\gamma_{\hat{\boldsymbol{q}}j} = \Gamma_{\boldsymbol{q}j}/\nu^5$ have been calculated by Tamura and Maris [15, 16] and Berke *et al* [17] for a number of substances in the approximation of a dispersionless but anisotropic non-linear elastic continuum. In this approximation the phonon frequencies, polarisation vectors and coupling coefficients V_3 are determined by the elastic constants of second and third order. For our calculations the expression of V_3 given in [17] has been used. The collinear and quasi-collinear decay discussed in [17] has not been taken into account in our calculations on the argument that, even for small values of the dispersion, its contribution to the damping constants can be expected to be negligibly small. $\gamma_{\hat{\boldsymbol{q}}j}$ is connected with $\gamma(\nu/\nu', \hat{\boldsymbol{q}}j, \hat{\boldsymbol{q}}'j')$ via the relation

$$4\gamma_{\hat{\boldsymbol{q}}'j'} = \sum_j \int \mathrm{d}\Omega \int_0^1 \mathrm{d}(\nu/\nu')\gamma(\nu/\nu', \hat{\boldsymbol{q}}j, \hat{\boldsymbol{q}}'j'). \tag{2.5}$$

For the sake of simplicity, the defect scattering is considered here only in the form of incoherent elastic scattering by mass defects. For this type of defect simple explicit expressions can be used [18]:

$$M(\hat{\boldsymbol{q}}j, \hat{\boldsymbol{q}}'j') = \sigma v_{\hat{\boldsymbol{q}}j}^{-3}(\hat{\boldsymbol{e}}(\hat{\boldsymbol{q}}j)\cdot\hat{\boldsymbol{e}}(\hat{\boldsymbol{q}}'j'))^2. \tag{2.6}$$

The quantity σ is proportional to the square of the mass excess and to the concentration of the defects. $\hat{\boldsymbol{e}}$ denotes the unit polarisation vector. Since the particle number is conserved in the scattering processes, the relation

$$M_{\hat{\boldsymbol{q}}'j'} = \sum_j \int \mathrm{d}\Omega\, M(\hat{\boldsymbol{q}}j, \hat{\boldsymbol{q}}'j') \tag{2.7}$$

holds.

3. Averaged phonon distributions and characteristic functions

Concerning the qualitative temporal behaviour of the phonon distribution function, the following frequency regimes can be distinguished. Since the phonon decay rate is proportional to a higher power of the frequency than the rate for elastic scattering, the latter may be neglected in a first approximation for phonons above a certain frequency. In this frequency regime, the longitudinal and fast-transverse components of an initial

non-equilibrium distribution give rise to fast decay cascades, in which slow-transverse phonons are generated. Apart from certain restricted areas of solid angle for the propagation directions, the spontaneous decay of the slow-transverse modes is negligible. On a timescale larger than that on which the fast cascades proceed, they will be down-converted by indirect processes, either via mode conversion due to elastic scattering [7, 8] or via up-conversion into longitudinal or fast-transverse modes, which may subsequently decay into phonons of lower frequency (see appendix 2). Because of the anisotropy of the rates in (2.2), even an initially isotropic phonon distribution will develop into an anisotropic distribution, i.e. the distribution function will depend on the propagation direction. In a first approximation, we will neglect this directional dependence and work with distribution functions averaged over the propagation directions,

$$f_j(\nu, t) = \int \mathrm{d}\Omega\, f_{\hat{q}j}(\nu, t). \tag{3.1}$$

We retain, however, the dependence on the polarisation. The transport equation for the averaged distribution function takes the form

$$\dot{f}_j(\nu, t) = -2\nu^5 \gamma_j f_j(\nu, t) + \sum_{j'} \int \mathrm{d}\nu' \nu'^4 \gamma(\nu/\nu', j, j') f_{j'}(\nu', t)$$
$$- \nu^4 M_j f_j(\nu, t) + \sum_{j'} \nu^4 M(j, j') f_{j'}(\nu, t). \tag{3.2}$$

The averages in (3.2) have to be performed in the following way:

$$A_j = [v_j^{-3}]^{-1} \int \mathrm{d}\Omega\, v_{\hat{q}j}^{-3} A_{\hat{q}j} \tag{3.3}$$

$$A(j, j') = [v_{j'}^{-3}]^{-1} \int \mathrm{d}\Omega' \int \mathrm{d}\Omega\, v_{\hat{q}'j'}^{-3} A(\hat{\boldsymbol{q}}j, \hat{\boldsymbol{q}}'j') \tag{3.4}$$

where $v_j^{-3} = \int \mathrm{d}\Omega\, v_{\hat{q}j}^{-3}$.

Here, A stands for γ and M, respectively. It can be shown easily that the permutation of the branches of the two generated phonons in the characteristic function $\gamma(\nu/\nu', j' \to j + j'')$ leads to the symmetry condition

$$\gamma(\nu/\nu', j' \to j + j'') = \gamma((\nu' - \nu)/\nu', j' \to j'' + j). \tag{3.5}$$

This allows one to derive a relation between the zeroth and first moment with respect to ν/ν':

$$\int_0^1 \mathrm{d}(\nu/\nu')\gamma(\nu/\nu', j' \to j + j'')$$
$$= \int_0^1 \mathrm{d}(\nu/\nu')(\nu/\nu')(\gamma(\nu/\nu', j' \to j + j'') + \gamma(\nu/\nu', j' \to j'' + j)) \tag{3.6}$$

and furthermore

$$\sum_{jj''} \int_0^1 \mathrm{d}(\nu/\nu')\gamma(\nu/\nu', j' \to j + j'') = 4\gamma_{j'}. \tag{3.7}$$

In an isotropic non-linear elastic medium, an initially isotropic distribution of acoustic

phonons will remain isotropic during the evolution of the cascade, and no additional approximation has to be made to arrive at equation (3.2). The characteristic functions occurring in this equation are expressed analytically in terms of the Lamé constants of second and third order in appendix 1.

As the maxima of the distribution functions of longitudinal and fast-transverse phonons move to lower frequencies with increasing time, they pass a frequency range where the spontaneous decay and the elastic scattering become equally important. With further decreasing frequency, the scattering becomes dominant leading to detailed balance between the phonon branches, i.e. if the distribution function $f_j(\nu, t)$ is expanded in eigen functions of the scattering operator

$$M(j, j') - \delta_{jj'} M_j \tag{3.8}$$

only the component corresponding to the eigenvector

$$v_j^{-3} f(\nu, t) \tag{3.9}$$

with eigenvalue zero will survive. It is then sufficient to work with the effective rate equation for this component

$$\dot{f}(\nu, t) = -2\nu^5 \gamma f(\nu, t) + \int \mathrm{d}\nu' \nu'^4 \gamma(\nu/\nu') f(\nu', t) \tag{3.10}$$

which contains the new averaged characteristic function

$$\gamma(\nu/\nu') = [v^{-3}]^{-1} \sum_{jj'} \gamma(\nu/\nu', j, j') v_{j'}^{-3} \tag{3.11}$$

where $v^{-3} = \Sigma_j v_j^{-3}$ and

$$4\gamma = \int_0^1 \mathrm{d}(\nu/\nu') \gamma(\nu/\nu'). \tag{3.12}$$

The discussion of the decay cascades and the equations determining their behaviour given so far relies on the fact that the defects in the system can be treated as individual incoherent scatterers for the acoustic phonons. For wavelengths of the phonons under consideration considerably larger than the average distance of the defects, this approximation is, however, expected to break down. For sufficiently low frequencies, the defective crystal will merely act as an effective elastic medium for the acoustic phonons, and concerning the relaxation of a non-equilibrium phonon distribution, the physical situation will be similar to that in the high-frequency regime described above.

With increasing phonon occupation number during the decay cascade, the linear approximation in the rate equations is no longer valid, and the non-linear terms in Peierls' collision operator have to be included [9] (see also appendix 2). These terms contain, apart from the occupation numbers, the characteristic functions introduced above, and no further integral kernels occur.

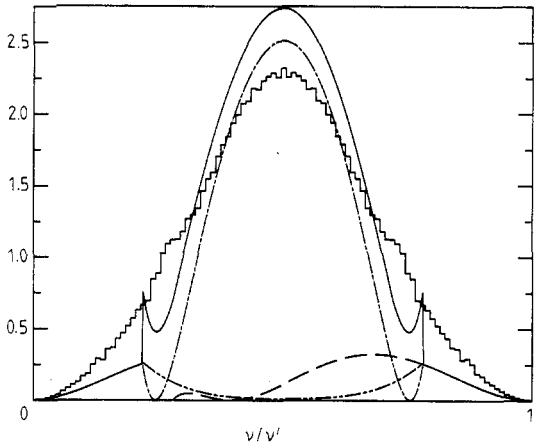

Figure 1. Normalised average characteristic function (histogram) for the anistropic medium in comparison with the normalised characteristic function obtained in the isotropic approximation (full curve), by averaging over the polarisations of the decay products. The other curves show the characteristics of each process (– – –, $L \rightarrow L + T_1$; ———, $L \rightarrow T_1 + T_1$; – – – –, $L \rightarrow T_2 + T_2$). The polarisation vectors of the transverse modes T_1 and T_2 are parallel and orthogonal to the $\boldsymbol{q} - \boldsymbol{q}'$ plane, respectively. The Lamé constants in the isotropic approximation [13] are: $\mu = 4.65$, $\lambda = 5.70$, $\beta = -9.90$, $\gamma = -5.83$.

4. Scaling properties

It has been shown by Kazakovtsev and Levinson [3], and later with different arguments by Happek *et al* [11, 12], that the solution of equation (3.10) after an initial time interval, which depends on the initial conditions, will have the following scaling form:

$$f(\nu, t) = t^{2/5} h(u) \tag{4.1}$$

where

$$u = (2\gamma t)^{1/5} \nu. \tag{4.2}$$

The latter authors have confirmed this scaling behaviour experimentally. The function $h(u)$ depends on the shape of the averaged characteristic function $\gamma(\nu/\nu')$. For a comparison with their experimental results, Happek *et al* have calculated the function $uh(u)$ from the transport equation (3.10) with the following ansatz for the averaged characteristic function:

$$\gamma(\nu/\nu') = N_\kappa (\nu/\nu')^\kappa (1 - \nu/\nu')^\kappa \tag{4.3}$$

where N_κ is determined by the normalisation. They found best agreement for the exponent $\kappa = 8$. The shape of the function on the right-hand side of equation (4.3) is, however, clearly different from the characteristic function shown in figure 1 and in particular does not show the correct behaviour for small ν/ν' derived by these authors and by Kazakovtsev and Levinson [3]. We have therefore calculated the scaling function for the energy distribution, $S(u) = uh(u)$, from the characteristic functions of figure 1, and in figure 2 we compare the result with the experimental data of Happek *et al* and their theoretical result for $S(u)$ obtained by using the ansatz (4.3). The fact that the characteristic functions used in our calculation show the correct behaviour for small values of ν/ν' is reflected in a better agreement with the experimental data in the small-u region. In the neighbourhood of the maximum of $S(u)$, however, the agreement is worse, while on the right wing of the curve, the result is inconclusive because of the scatter of the experimental data.

A scaling form for the solution of the rate equations can also be derived for the case of absent defect scattering. In showing this, we confine ourselves to the isotropic case, where only the spontaneous decay of the longitudinal modes (L) has to be taken into

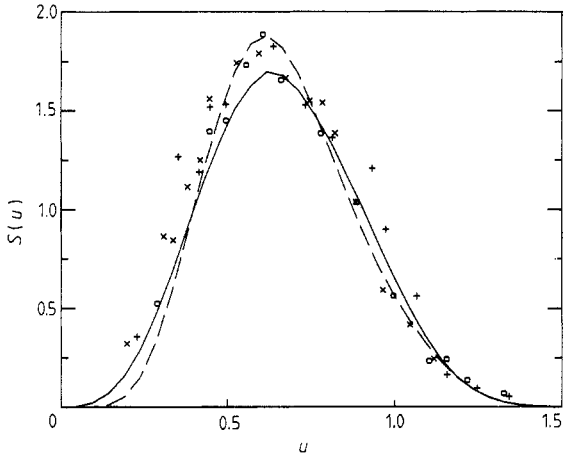

Figure 2. The function $S(u) = uh(u)$ obtained from the averaged characteristic function (1) of figure 1 in comparison with the experimental data of references [11] and [12] (from the measured spectral distribution after 7×10^8 s (×), 17×10^8 s (+) and 50×10^8 s (○). The broken curve is obtained by replacing the averaged characteristic in equation (3.10) by the ansatz (4.3).

account, while the distribution function of the transverse phonons (T) is monotonically increasing with time. After an initial time interval, the longitudinal part of the distribution function takes the form

$$f_L(\nu, t) = t^{\mu/5} h_L(u) \tag{4.4}$$

where

$$u = (2\gamma_L t)^{1/5} \nu. \tag{4.5}$$

The energy initially deposited in the system of longitudinal phonons is transferred to transverse phonons during the cascade according to the power law

$$E_L(t) \sim t^{(\mu-2)/5}. \tag{4.6}$$

The exponent μ depends in a non-trivial way on the relative strengths of the different decay processes. By using the energy conservation for the total system of longitudinal and transverse phonons, it can be shown that μ is related to the first (M_1) and sixth (M_6) moments of the function h_L via $(\mu - 2)/5 = -\gamma(\mathrm{L}, \mathrm{T})\gamma_L^{-1} M_6 M_1^{-1}$ where

$$\gamma(\mathrm{L}, \mathrm{T}) = \tfrac{1}{2} \int_0^1 \mathrm{d}(\nu/\nu')(\nu/\nu')\gamma(\nu/\nu', \mathrm{L}, \mathrm{T}). \tag{4.7}$$

With the characteristics calculated for the decay of longitudinal phonons in CaF_2, we obtain $\mu = -2.24$.

5. Numerical calculations for CaF_2

While in the isotropic case only longitudinal phonons decay and the two transverse branches are degenerate, i.e. L → T + T and L → T + L, there is a greater variety of decay processes in anisotropic media. The following types of processes have been taken into account in the numerical calculations:

L → ST + ST L → ST + FT L → ST + L

L → FT + FT L → FT + L

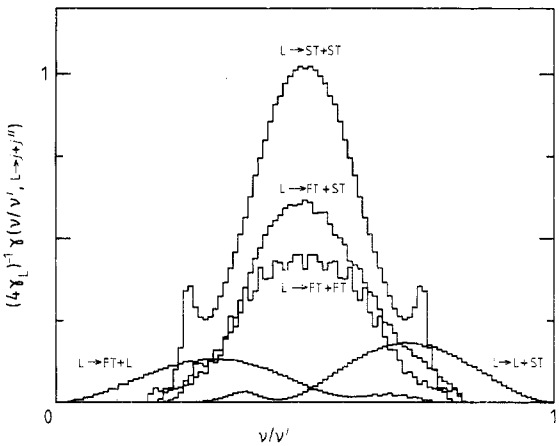

Figure 3. Characteristic functions of longitudinal phonons. The parameters used for the data in this and the following figure are listed in table 1.

$$\mathrm{FT} \longrightarrow \mathrm{ST} + \mathrm{ST} \qquad \mathrm{FT} \longrightarrow \mathrm{ST} + \mathrm{FT} \qquad \mathrm{FT} \longrightarrow \mathrm{ST} + \mathrm{L}.$$

The intra-branch decay of the longitudinal mode occurs only as a collinear process in the non-dispersive approximation and is forbidden in the presence of normal dispersion. It has been demonstrated [17, 19] that realistic values for the dispersion cause the intra-branch decay of transverse modes to be negligible. The decay $\mathrm{ST} \longrightarrow \mathrm{ST} + \mathrm{FT}$ has only been found in small parts of solid angle very close to the direction of degeneracy of the two transverse branches. In our numerical calculations, it has been disregarded. In the anisotropic case the characteristic functions have been calculated numerically and are presented in the form of histograms. The zeros in the argument of the delta function with respect to k in equation (2.4) have been determined with the help of the analytic expressions for the sound velocities given by Every [20, 21]. For the integration over solid angle $\mathrm{d}\Omega'$, we have used a gaussian algorithm with meshes of several thousands of points adapted to the shape of the integration area. For the integration over $\mathrm{d}\Omega$, 17 points have been positioned in the irreducible segment of solid angle.

The experimental elastic constants enter the matrix element V_3 as input parameters. Unfortunately, the third-order elastic constants at liquid helium temperature are not available. In order to avoid numerical inaccuracies due to compensations in linear combinations of second- and third-order elastic constants as far as possible, we have taken the room-temperature data set for these combinations [22]. For the frequencies and eigenvectors, however, the low-temperature second-order elastic constants [23] have been used, because the density of states may depend sensitively on them.

The characteristic function is proportional to the probability for a phonon of frequency ν' and polarisation j' to decay per unit time into two phonons with one in the frequency interval $\mathrm{d}\nu$ and polarisation j. The area under the normalised characteristic function $\gamma(\nu/\nu', j' \rightarrow j + j'')(4\gamma_{j'})^{-1}$ for a certain branch combination represents the relative probability for this type of decay process to occur. In figure 3 the characteristic functions for longitudinal phonons are shown. The anisotropy has been fully taken into account. The basic features of the corresponding curves for the isotropic medium (figure 1) are maintained, but due to the average over the propagation direction the characteristics have a smoother shape. As in the isotropic case there is a cut-off at high and low frequencies for the decay into transverse phonons, and a single cut-off for the decay into a longitudinal and a transverse phonon. In the anisotropic medium the decay into transverse phonons is no more symmetric because of the non-symmetric process

Table. 1. Input parameters for CaF_2†.

Low-temperature elastic moduli of reference [23]			High-temperature elastic moduli of reference [22]		
$C_{11} = 17.4$	$C_{12} = 5.6$	$C_{44} = 3.593$	$C_{11} = 16.42$	$C_{12} = 4.398$	$C_{44} = 3.37$
			$C_{111} = -124.6$	$C_{112} = -40.0$	$C_{123} = -25.4$
			$C_{144} = -12.4$	$C_{166} = -21.4$	$C_{456} = -7.48$

† Units in 10^{10} N m^{-2}. Mass density $\rho = 3210.7$ kg m^{-3}.

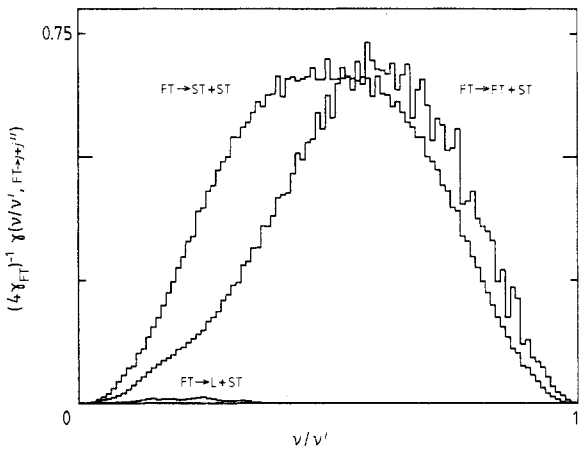

Figure 4. Characteristic functions of fast-transverse phonons.

L⟶ ST + FT. Figure 4 shows the characteristic functions for the FT phonons. These functions vanish in the isotropic case. The dominant decay processes into transverse phonons cover the complete spectrum and do not present such strong features as in the preceding case (figure 3). The decay into longitudinal phonons plays a minor role. Compared with figure 3, the structure of the non-symmetric decay into longitudinal phonons appears on the other side of the frequency spectrum, while FT and ST phonons are generated in preference on the same side of the frequency scale. For the decay of a FT phonon, for example, longitudinal phonons are generated only at frequencies lower than the cut-off frequency, while they occur at frequencies higher than the cut-off frequency for a decay of a longitudinal phonon.

The system of coupled integro-differential equations (3.2) has been solved with the method of Runge and Kutta. Energy conservation is verified in each step. Figures 5(*a*)–(*c*) show the temporal evolution of the distribution functions in the absence of scattering. We start from a monochromatic source of longitudinal phonons of frequency $\nu_0 =$ 1THz. The initial state has not been shown in the diagrams. In the first time steps, the distribution function is dominated by the shape of the characteristic function. Due to the ν^5 law, the high-frequency longitudinal phonons decrease rapidly. The decay of fast-transverse phonons proceeds much more slowly because of their smaller damping. The slow-transverse phonons do not participate in the decay process. Their lifetime is in our approximation infinite, $\gamma_{ST} = 0$. Our numerical calculations for the reduced damping constants of the longitudinal and fast-transverse branches yield

$$\gamma_L = 2.7 \times 10^{-55} s^4 \qquad \gamma_{FT} = 5.0 \times 10^{-56} s^4. \tag{5.1}$$

Already after the first time interval of 4×10^{-5}s, which corresponds to the lower end of

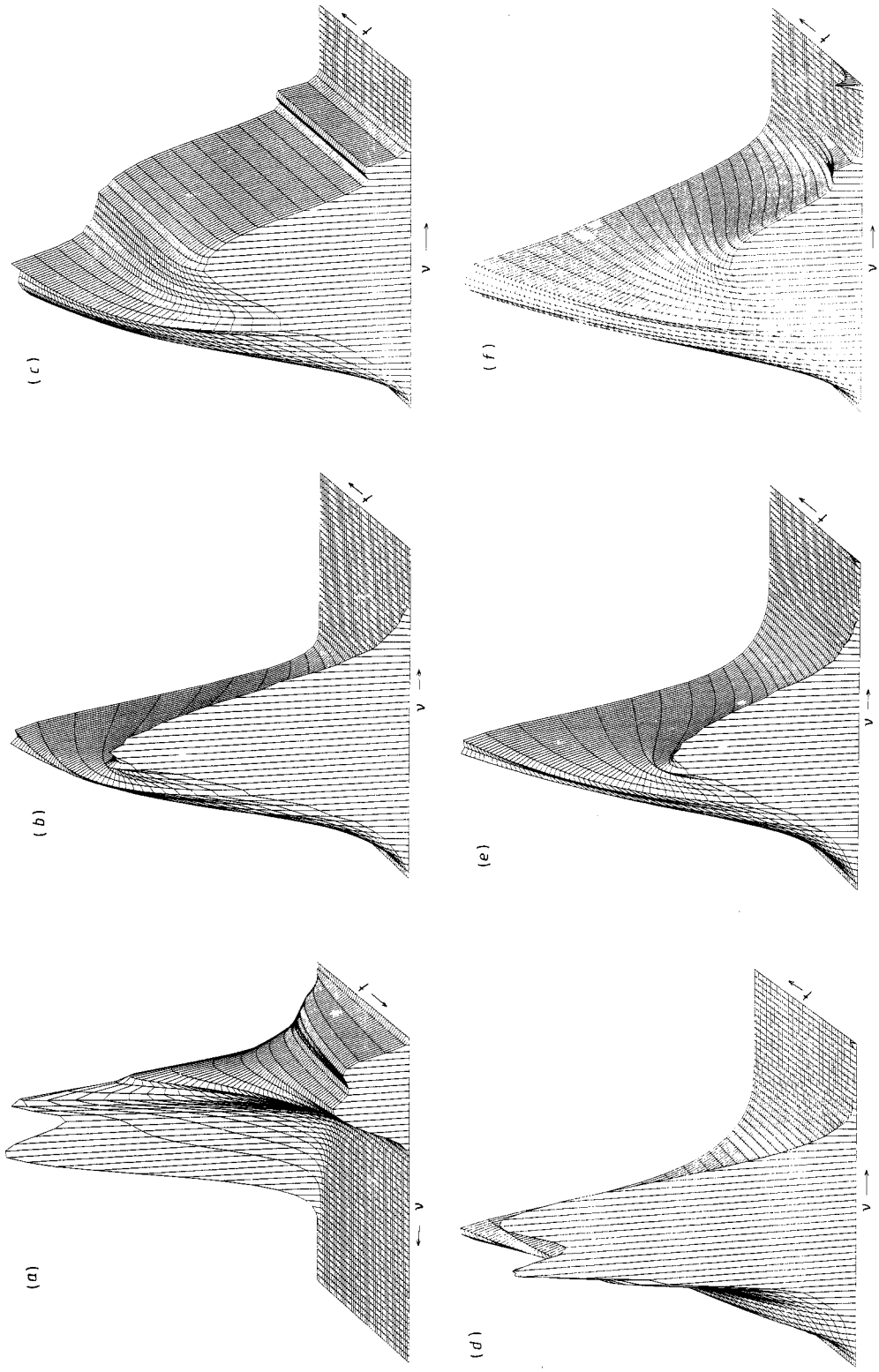

Figure 5. The temporal evolution of the frequency distribution function $f_t(\nu, t)$, $\nu \in [0, 1\ \text{THz}]$, $t \in [0, 2 \times 10^{-3}\ \text{s}]$ of L ((*a*), (*d*)), FT ((*b*), (*e*)) and ST ((*c*), (*f*)) phonons in a perfect crystal ((*a*)–(*c*)) is compared with a crystal containing elastic scattering centres ((*d*)–(*f*)).

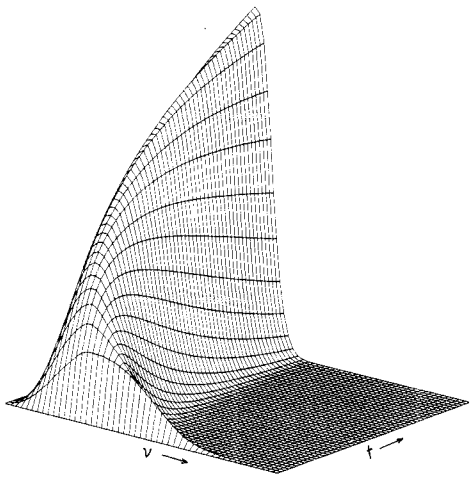

Figure 6. Distribution function $f(\nu, t)$, $\nu \in [0, 1\,\mathrm{THz}]$, $t \in [0, 8 \times 10^{-3}\,\mathrm{s}]$ in the detailed balance regime.

the timescale in figure 5, the percentage energy distribution is (3%L, 35%FT, 62%ST). At this stage the energy distribution of FT phonons has already passed its maximum. For long times all phonons will be converted into non-decaying ST phonons. At the last time step in figure 5, the energy distribution is approximately (0%L, 14%FT, 86%ST). The longitudinal phonons have nearly completely disappeared.

The evolution of the distribution function for a real crystal containing elastic scattering centres in the form of impurities and isotopes is shown in figures 5(*d*)–(*f*). Our numerical calculations have been performed with a ratio of decay and scattering rates of $M_L(\gamma_L \nu_0)^{-1} = 0.03$. The strength of the mode conversion is determined by the scalar products of the polarisation vectors, which may be expressed by the ratios

$$\tilde{M}(\mathrm{FT}, \mathrm{ST}) : \tilde{M}(\mathrm{L}, \mathrm{ST}) : \tilde{M}(\mathrm{L}, \mathrm{FT}) = 4.31 : 0.76 : 0.55. \tag{5.2}$$

Here, we have defined

$$\tilde{M}(j, j') = M(j, j') v_{j'}^{-3}. \tag{5.3}$$

Furthermore,

$$v_{\mathrm{ST}}^{-3} : v_{\mathrm{FT}}^{-3} : v_{\mathrm{L}}^{-3} = 6.2 : 4.4 : 0.8. \tag{5.4}$$

The peaks in the uppermost frequency interval of transverse phonons result from scattering processes of the monochromatic source of longitudinal phonons. Slow-transverse phonons decay indirectly via mode conversion [7, 8]. At low frequencies the distribution function is governed by scattering, while at high frequencies decay dominates, in accordance with the qualitative discussion in § 3. The energy distribution after the initial time interval still remains the same as in the preceding case. At the last time step, however, scattering is effective (1%L, 25%FT, 74%ST). In the regime of detailed balance, the energy is distributed over the branches according to the density of states, in the present case (6.8%L, 38.69%FT, 54.51%ST).

6. Conclusions

In summary, it has been shown that the decay cascades of THz phonons in CaF_2 observed by Happek *et al* can be described in terms of non-linear elasticity theory. In

this description, the anisotropy of the phonon–phonon interactions, as given by the experimental elastic constants of second and third order, is fully taken into account and no adjustable parameters have been introduced. Furthermore, the temporal evolution of the spectral distribution over the phonon branches has been studied numerically, using characteristic functions for the phonon decay averaged over directions. The qualitative differences of the phonon dynamics in the presence and absence of elastic scatterers in the form of mass defects have been established, and several predictions made by Levinson and co-workers have been confirmed. A further scaling law has been found for the phonon distribution function in isotropic elastic media without elastic scattering. The calculations presented here do not cover the regime of very low frequencies or very high defect concentration, where the approximation of incoherent scattering, made throughout this paper, is not applicable. They can, however, easily be extended to include effects of a finite ambient temperature. Further theoretical work is desirable to study effects of phonon dispersion, which influences especially the anharmonic decay of the slow-transverse phonons. The properties of the latter are of interest in regimes of low frequency.

Acknowledgments

We would like to thank Professor K F Renk for stimulating discussions. One of us (APM) gratefully acknowledges financial support from the Deutsche Forschungsgemeinschaft.

Appendix 1. Characteristic functions for isotropic elastic media

For isotropic non-linear elastic media, the characteristic functions $\gamma(\nu/\nu', \hat{\boldsymbol{q}}j, \hat{\boldsymbol{q}}'j')$, which enter equation (3.2), have been studied numerically by Obermayer [13]. They can be calculated from the following analytical formulae in terms of the Lamé constants of second and third order. For the derivation of these expressions, one may proceed in a way similar to the calculation of the damping constants by Tamura [15], and the definition of the Lamé constants is the same as in reference [15]. To simplify the notation, we introduce the abbreviations

$$n = \nu/\nu' \tag{A.1}$$

$$r = v_{\mathrm{L}}/v_{\mathrm{T}} \tag{A.2}$$

where v_{L} and v_{T} are the longitudinal and transverse sound velocities. The characteristics can then be expressed in the form

$$\gamma(n, j, \mathrm{L}) = \sum_{j'} \gamma(n, \mathrm{L} \rightarrow j + j') \qquad \gamma(n, \mathrm{L} \rightarrow j + j') = N\tilde{\gamma}(n, \mathrm{L} \rightarrow j + j') \tag{A.3}$$

$$\tilde{\gamma}(n, \mathrm{L} \rightarrow \mathrm{L} + \mathrm{T}) = [C_1 n(1+n)x_{\mathrm{L}}(1 - x_{\mathrm{L}}^2)^{1/2}]^2 r^{-4} \tag{A.4}$$

$$\tilde{\gamma}(n, \mathrm{L} \rightarrow \mathrm{T} + \mathrm{L}) = \tilde{\gamma}(1 - n, \mathrm{L} \rightarrow \mathrm{L} + \mathrm{T}) \tag{A.5}$$

$$\tilde{\gamma}(n, \mathrm{L} \rightarrow \mathrm{T} + \mathrm{T}) = \tilde{\gamma}(n, \mathrm{L} \rightarrow \mathrm{T}_1 + \mathrm{T}_1) + \tilde{\gamma}(n, \mathrm{L} \rightarrow \mathrm{T}_2 + \mathrm{T}_2) \tag{A.6}$$

where

$$\tilde{\gamma}(n, \mathrm{L} \rightarrow \mathrm{T}_1 + \mathrm{T}_1) = \{[C_2(rn - x_\mathrm{T})^2 - C_3(1 - x_\mathrm{T}^2)]n(1-n)^{-1}\}^2 \tag{A.7}$$

$$\tilde{\gamma}(n, \mathrm{L} \rightarrow \mathrm{T}_2 + \mathrm{T}_2) = [C_4(x_\mathrm{T} - rn) + C_5 x_\mathrm{T}(1 - x_\mathrm{T} rn)]^2 r^2 n^2. \tag{A.8}$$

The quantities x_L and x_T are given by

$$x_\mathrm{L} = (1/2n)[1 + n^2 - (1-n)^2 r^2] \tag{A.9}$$

$$x_\mathrm{T} = (1/2n)[r^{-1} - r(1-2n)]. \tag{A.10}$$

The factor N can be calculated from

$$N = 4\pi^5 \hbar \rho^{-3}. \tag{A.11}$$

Here, ρ is the mass density. An analytic expression for the reduced damping constant γ_L of longitudinal phonons due to the spontaneous decay can be found in reference [17]. The quantities $C_1, \ldots, C_5$ are given in terms of the Lamé constants via

$$C_1 = 2\beta + 4\gamma + \lambda + 3\mu \tag{A.12}$$

$$C_2 = \beta + \lambda + 2(\gamma + \mu) \tag{A.13}$$

$$C_3 = \beta + 2\gamma + \lambda \tag{A.14}$$

$$C_4 = \beta + \lambda \tag{A.15}$$

$$C_5 = 2(\gamma + \mu). \tag{A.16}$$

The Lamé constants β and γ of Tamura [15] are equal to ν_2 and ν_3 of Thurston and Brugger [24].

Appendix 2. Temporal evolution of transverse phonon occupation numbers via up-conversion

In the high-frequency regime, where the impurity scattering rate is much smaller than the damping rate due to spontaneous decay, the longitudinal and fast-transverse components of the decay cascade move rapidly to lower frequencies generating also slow-transverse phonons in the decay processes, which cannot decay directly via three-phonon interaction. It has been pointed out by Guseinov and Levinson [7, 8] that these phonons can decay indirectly on a longer timescale via mode conversion due to impurity scattering into directly decaying phonons. An effective equation for the temporal evolution of the occupation numbers of the non-decaying modes and a scaling law for their dependence on time and frequency have been derived by these authors. In the absence of incoherent scatterers, this type of indirect decay is, however, not possible. A redistribution of the occupation numbers of the non-decaying modes can then be caused by up-conversion into directly decaying phonons. To take account of these processes, rate equations for the phonon occupation numbers have to be considered, which contain the complete non-linear Peierls collision integral [25]

$$\frac{\partial}{\partial t} n_{\hat{q}j}(\nu) = \tfrac{1}{2}\nu^4 \sum_{j'j''} \int \mathrm{d}\Omega' \int_0^\nu \mathrm{d}\nu' \gamma(\nu'/\nu, \hat{\boldsymbol{q}}j \rightarrow \hat{\boldsymbol{q}}'j' + \hat{\boldsymbol{q}}''j'')$$

$$\times \{-n_{\hat{q}j}(\nu)[n_{\hat{q}'j'}(\nu') + n_{\hat{q}''j''}(\nu - \nu') + 1] + n_{\hat{q}'j'}(\nu') n_{\hat{q}''j''}(\nu - \nu')\}$$

$$+\sum_{j'j''}\int \mathrm{d}\Omega' \frac{v_{\hat{q}j}^3}{v_{\hat{q}'j'}^3}\int_\nu^\infty \mathrm{d}\nu'\nu'^4(\nu'/\nu)^2\gamma(\nu/\nu', \hat{q}'j' \to \hat{q}j + \hat{q}''j'')$$

$$\times\{n_{\hat{q}'j'}(\nu')[n_{\hat{q}j}(\nu) + n_{\hat{q}''j''}(\nu'-\nu) + 1] - n_{\hat{q}j}(\nu)n_{\hat{q}''j''}(\nu'-\nu)\} \qquad (A.17)$$

where $\hat{q}'' = \widehat{\hat{q} - (v_{\hat{q}j}/v_{\hat{q}'j'})(\nu'/\nu)\hat{q}'}$. We now confine ourselves to the isotropic case, where only the longitudinal phonons decay directly. To derive an effective equation for the occupation numbers of the transverse phonons, n_T, we retain only terms up to second order in n_T and eliminate the longitudinal occupation numbers in the same way as has been done in references [7] and [8]. This finally leads to an equation of the form

$$\frac{\partial}{\partial t}n_T(\nu) = \int_\nu^\infty \mathrm{d}\nu'\nu'^4\int_0^\infty \mathrm{d}\nu'' G_1(\nu''/\nu', \nu/\nu')n_T(\nu'')n_T(\nu'-\nu'')$$

$$-\int_\nu^\infty \mathrm{d}\nu'\nu'^4 G_2(\nu/\nu')n_T(\nu)n_T(\nu'-\nu). \qquad (A.18)$$

The kernels G_1 and G_2 depend only on the frequency ratios.

References

[1] For reviews see: Bron W E 1985 *Nonequilibrium Phonon Dynamics* ed. W E Bron (New York: Plenum)
Renk K F 1985 *Nonequilibrium Phonon Dynamics* ed. W E Bron (New York: Plenum)
Ulbrich R G 1985 *Nonequilibrium Phonon Dynamics* ed. W E Bron (New York: Plenum)
[2] Kazakovtsev D V and Levinson Y B 1978 *Sov. Phys.–JETP Lett.* **27** 181
[3] Kazakovtsev D V and Levinson Y B 1979 *Phys. Status Solidi* b **96** 117
[4] Levinson Y B 1980 *Sov. Phys.–JETP* **52** 704
[5] Levinson Y B 1980 *Solid State Commun.* **36** 73
[6] Esipov S E and Levinson Y B 1981 *Sov. Phys.–JETP Lett.* **34** 210
[7] Guseinov N M and Levinson Y B 1983 *Solid State Commun.* **45** 371
[8] Guseinov N M and Levinson Y B 1983 *Sov. Phys.–JETP* **58** 452
[9] Schaich W L 1984 *Solid State Commun.* **49** 55
[10] Wilson T E and Schaich W L 1984 *Solid State Commun.* **50** 3
[11] Happek U, Renk K F, Ayant Y and Buisson R 1986 *Phonon Scattering in Condensed Matter V* ed. A C Anderson and J P Wolfe (Berlin: Springer) p 347
[12] Happek U, Ayant Y, Buisson R and Renk K F 1987 *Europhys. Lett.* **3** 1001
[13] Obermayer P unpublished work
[14] Baumgartner R, Engelhardt M and Renk K F 1981 *Phys. Rev. Lett.* **47** 1403
[15] Tamura S 1985 *Phys. Rev.* B **31** 2574
[16] Tamura S and Maris H J 1985 *Phys. Rev.* B **31** 2595; 1985 *Solid State Commun.* **54** 395
[17] Berke A, Mayer A P and Wehner R K 1988 *J. Phys. C: Solid State Phys.* **21** 2305
[18] Klemens P G 1958 *Thermal Conductivity and Lattice Vibrational Modes, Solid State Physics* vol 7, ed. F Seitz and D Turnbull
[19] Mayer A P 1987 *J. Phys. C: Solid State Phys.* **20** L201
[20] Every A G 1979 *Phys. Rev. Lett* **42** 1065
[21] Every A G 1981 *Phys. Rev.* B **24** 3456
[22] Alterovitz S and Gerlich D 1968 *Phys. Rev.* **184** 999
[23] Huffman D R and Norwood M H 1960 *Phys. Rev.* **117** 709
[24] Thurston R N and Brugger K 1964 *Phys. Rev.* **133** A1604
[25] Peierls R E 1955 *Quantum Theory of Solids* (Oxford: Clarendon)